

Vyacheslav E. Zavlin

Studying Millisecond Pulsars in X-rays

arXiv:astro-ph/0608210v2 17 Aug 2006

Received: date / Accepted: date

Abstract Millisecond pulsars represent an evolutionarily distinct group among rotation-powered pulsars. Outside the radio band, the soft X-ray range ($\sim 0.1\text{--}10$ keV) is most suitable for studying radiative mechanisms operating in these fascinating objects. X-ray observations revealed diverse properties of emission from millisecond pulsars. For the most of them, the bulk of radiation is of a thermal origin, emitted from small spots (polar caps) on the neutron star surface heated by relativistic particles produced in pulsar acceleration zones. On the other hand, a few other very fast rotating pulsars exhibit almost pure nonthermal emission generated, most probably, in pulsar magnetospheres. There are also examples of nonthermal emission detected from X-ray nebulae powered by millisecond pulsars, as well as from pulsar winds shocked in binary systems with millisecond pulsars as companions. These and other most important results obtained from X-ray observations of millisecond pulsars are reviewed in this paper, as well as results from the search for millisecond pulsations in X-ray flux of the radio-quiete neutron star RX J1856.5–3754.

Keywords X-rays · Neutron stars · Millisecond pulsars

PACS 95.85.Nv · 97.10.Qh · 97.60.Jd · 97.60.Gb

1 Introduction

Millisecond pulsars (MSPs) significantly differ in properties from other (ordinary) radio pulsars. First of all, MSPs possess very short and stable spin periods, $P \lesssim 50$ ms, with extremely small period derivatives, $\dot{P} \lesssim 10^{-18}$ s s $^{-1}$. These two main parameters separate MSPs from the majority of other pulsars, as illustrated in the $P\text{--}\dot{P}$

V.E. Zavlin
Space Science Laboratory, NASA MSFC SD50, Huntsville,
AL 35805, USA
Tel.: +1-256-961-7463
Fax: +1-256-961-7522
E-mail: vyacheslav.zavlin@msfc.nasa.gov

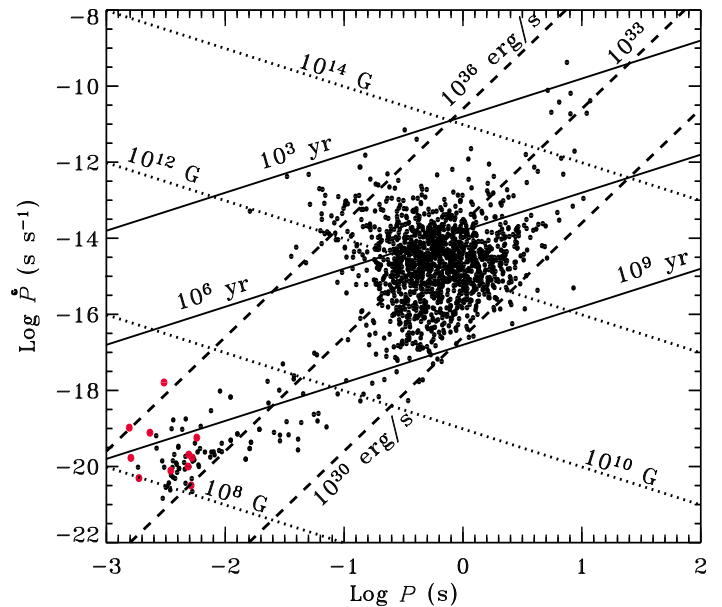


Fig. 1 $P\text{--}\dot{P}$ diagram for about 1,500 radio pulsars (dots). Millisecond pulsars are located in the lower-left corner of the diagram. The pulsars from Table 1 and 3 are shown with red dots. Straight lines correspond to constant values of pulsar characteristic age $\tau = 10^3, 10^6$ and 10^9 yr, surface magnetic field $B_{\text{surf}} = 10^8, 10^{10}, 10^{12}$ and 10^{14} G, and spin-down energy $\dot{E} = 10^{30}, 10^{33}$ and 10^{36} erg s $^{-1}$.

diagram¹ shown in Figure 1. According to the conventional pulsar magnetic-braking model, MSPs are very old neutron stars, with characteristic ages $\tau = P/2\dot{P} \sim 0.1\text{--}10$ Gyr, and low surface magnetic fields $B_{\text{surf}} \simeq 3.2 \times 10^{19} (P\dot{P})^{1/2} \lesssim 10^{10}$ G (see Fig. 1). They were presumably spun up by angular momentum transfer during a mass accretion phase in binary systems² (e.g., Alpar et al. 1982), and their low values of B_{surf} could be explained

¹ Based on the pulsar catalog provided by the Australia Telescope National Facility (Manchester et al. 2005) and available at <http://www.atnf.csiro.au/research/pulsar>.

² It is why MSPs are often called “recycled” pulsars.

Table 1 Main parameters of eight MSPs

PSR	P (ms)	d (kpc)	τ (Gyr)	$\log \dot{E}$ (erg s $^{-1}$)
B1937+21	1.56	3.57	0.24	36.0
B1957+20	1.61	2.49	2.24	35.0
J0218+4232	2.32	2.67	0.48	35.4
B1821-24	3.05	3.09	0.03	36.3
J0030+0451	4.87	0.32	7.71	33.5
J2124-3358	4.93	0.27	6.01	33.6
J1024-0719	5.16	0.39	> 27.25	< 32.9
J0437-4715	5.76	0.14	6.51	33.5

by the Ohmic and/or accretion-induced decay of magnetic field (see Cumming 2005 and references therein). Discoveries of several accretion-driven binary MSPs, first of all the famous pulsar SAX J1808.4-3658 with $P \simeq 2.5$ ms, support this hypothesis (see, e.g., Wijnands 2004 for a review on accreting MSPs).

Since the discovery of the first fast rotating pulsar B1937+21 by Backer et al. (1982), MSPs have been extensively searched for and studied in radio domain. Currently, about 130 MSPs are known (Manchester et al. 2005). Outside the radio band, as MSPs are intrinsically faint at optical wavelengths and most of them ($\sim 80\%$) reside in binary systems with optically brighter white dwarf companions, the soft X-ray energy range (~ 0.1 – 10 keV) is the main source of information on these pulsars. The detection of pulsed X-ray emission from the brightest (and nearest) MSP J0437-4715 with *ROSAT* (Becker & Trümper 1993) initiated a series of dedicated X-ray observations of these intriguing objects in 90’s with this satellite and also *ASCA*, *BeppoSAX* and *RXTE*. Later on this observational “relay” has been continued with *Chandra* and *XMM-Newton*. So far, firm X-ray detections have been reported for about three dozens of isolated (solitary, or non-accreting if in binaries) MSPs. The majority of these objects are located in globular clusters (mostly 47 Tuc — see Bogdanov et al. 2006). This paper mainly concentrates on eight MSPs, listed in Table 1, with available detailed information on properties of detected X-ray emission. Besides P and τ , Table 1 gives estimates on the distances to these objects, d (inferred from either pulsar parallaxes or dispersion measures and the NE2001 galactic electron density model by Cordes & Lazio 2003)³, and on their spin-down energies, $\dot{E} = 4\pi^2 I P^{-3} \dot{P}$ (assuming a standard neutron star moment of inertia, $I = 10^{45}$ g cm 2). Note that for PSR J1024-0719 the intrinsic period derivative is not well determined, $\dot{P} < 3 \times 10^{-21}$ s s $^{-1}$ (Hotan, Bails &

Ord 2006), that results in the lower and upper limits on τ and \dot{E} , respectively.

Generally, X-ray emission from radio pulsars consists of two different components, thermal and nonthermal, generated on the neutron star surface or in its vicinity. The nonthermal component is usually described by a power-law (PL) spectral model and attributed to radiation produced by synchrotron and/or inverse Compton processes in the pulsar magnetosphere, whereas the thermal emission can originate from either the whole surface of a cooling neutron star or small hot spots around the magnetic poles (polar caps; PCs) on the star surface, or both. As predicted by virtually all pulsar models, these PCs can be heated up to X-ray temperatures (~ 1 MK) by relativistic particles generated in pulsar acceleration zones. A conventional assumption about the PC radius is that it is close to the radius within which open magnetic field lines originate from the pulsar surface, $\sim [2\pi R_{\text{NS}}^3/cP]^{1/2} \simeq 2[P/5\text{ms}]^{-1/2}$ km (for a neutron star radius $R_{\text{NS}} = 10$ km). In case of MSPs, the entire surface at a neutron star age of ~ 1 Gyr is too cold, $\lesssim 0.1$ MK, to be detectable in X-rays (although it may be seen in the *UV/FUV* band — see Sec. 6). Therefore, only nonthermal (magnetospheric) and/or thermal PC radiation is expected to be observed in X-rays from these objects. In addition to the radiation produced by MSPs themselves, nonthermal emission from pulsar-wind nebulae (PWNe) associated with MSPs moving at supersonic velocities ($\gtrsim 100$ km s $^{-1}$) through interstellar medium may be detected. Another source of nonthermal X-ray radiation generated in binary systems can be an intra-binary shock formed where the pulsar wind and matter from the stellar component collide (Arons & Tavani 1993), although such a component would be hardly separated from radiation produced by the pulsar itself (unless properties of the nonthermal emission varies with orbital phase).

The MSPs in Table 1 belong to two distinct groups: those which emit almost pure nonthermal radiation and those with a predominantly thermal PC component. The next two Sections provides details on the X-ray properties of these objects. Section 4 is devoted to three X-ray emitting MSPs whose properties remain uncertain. X-ray PWNe powered by MSPs are briefly discussed in Section 5. A summary is given in Section 6.

2 Nonthermally emitting MSPs

Of the MSPs listed in Table 1, these are PSRs B1937+21, B1957+20, J0218+4232, and B1821-24. They are characterized by large values of spin-down energy, $\dot{E} > 10^{35}$ erg s $^{-1}$, and shorter spin periods, $P < 3.1$ ms. PSR J0218+4232 is also one of few γ -pulsars known (Kuiper et al. 2000). X-ray observations of these MSPs revealed their nonthermal spectra, albeit with different photon indices Γ . Figures 2–5 show the spectra detected with

³ For the MSPs of the second group in Table 1 (with $d < 1$ kpc), the distance estimates obtained from the pulsar parallaxes and those inferred from their dispersion measures agree well with each other (see Hotan, Bails & Ord 2006 and Lommen et al. 2006).

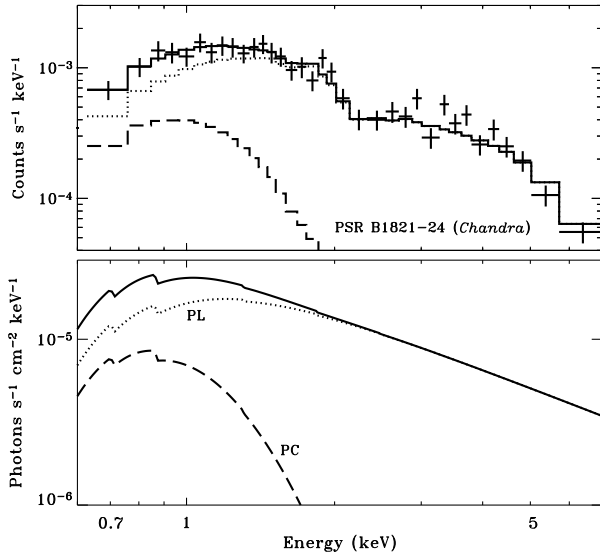


Fig. 2 X-ray spectrum of PSR B1821-24 as detected with the *Chandra* ACIS-S instrument (crosses) fitted with a PL model of $\Gamma = 1.2$ (dotted curves) plus a possible PC component (dashes). See also Becker et al. (2003).

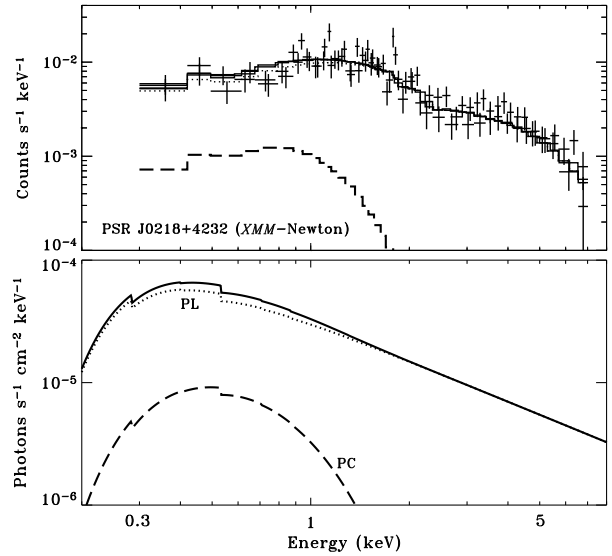


Fig. 4 Same as in Fig. 2 for PSR J0218+4232 (as detected with the *XMM-Newton* EPIC-MOS instruments) and a PL model of $\Gamma = 1.1$ (see also Webb, Olive & Barret 2004).

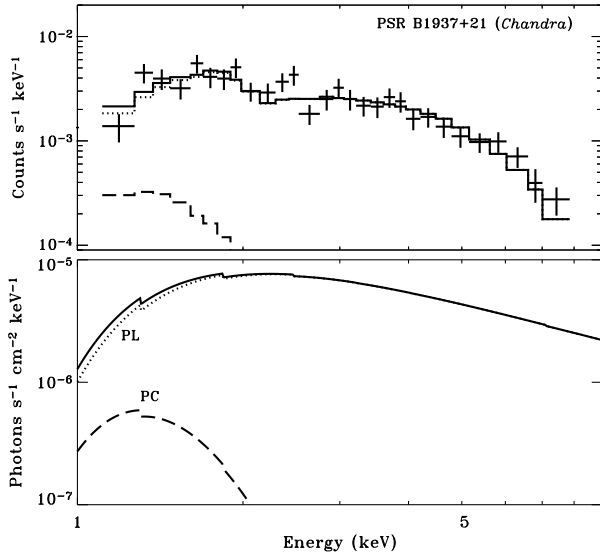


Fig. 3 Same as in Fig. 2 for PSR B1937+21 and a PL model of $\Gamma = 1.2$ (see also Kuiper et al. 2006).

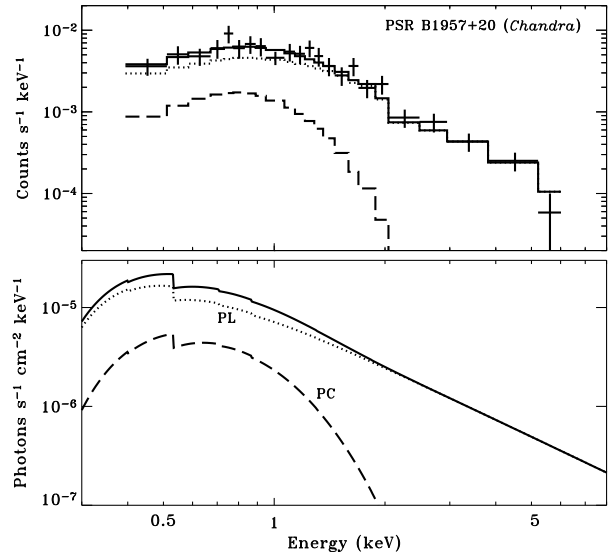


Fig. 5 Same as in Fig. 2 for PSR B1957+20 and a PL model of $\Gamma = 1.9$. (Note that the detected flux can contain a contribution from a possible intrabinary shock — see Sec. 2 and Stappers et al. 2003 for more details.)

Chandra and/or *XMM-Newton* from these MSPs. Although the spectral data on these pulsars do not formally require any other component (in addition to a PL), one cannot exclude that there is also a contribution of thermal PC emission in the detected X-ray fluxes, as indicated in Figures 2–5. For PSRs B1821-24, J0218+4232, and B1937+21 the measured photon indices are $\Gamma \simeq 1.1$ – 1.2 . The spectrum of PSR B1957+20, was found to be much steeper, with $\Gamma \simeq 1.9$ (although the X-ray radiation of this pulsar can consist of two component — see below). Note that these estimates on Γ are derived for the phase-integrated fluxes, whereas the observational data on PSRs J0218+4232 and B1937+21 indicate that

the spectral slope may change with pulsar rotational phase (see Webb, Olive & Barret 2004 and Nicastro et al. 2004). However, much more sensitive observations are required to confirm this effect. Regarding the X-ray spectrum of PSR B1821-24 (located in the globular cluster M28), Becker et al. (2003) speculated that there is a marginal evidence for an emission line around 3.3 keV (see also Fig. 2). If this feature is real⁴, it could be interpreted as cyclotron emission from an optically thin

⁴ There is no indication of a feature at this photon energy in the spectra of PSRs B1957+20 and B1937+21 detected with the same *Chandra* ACIS-S instrument (Figs. 3 and 5).

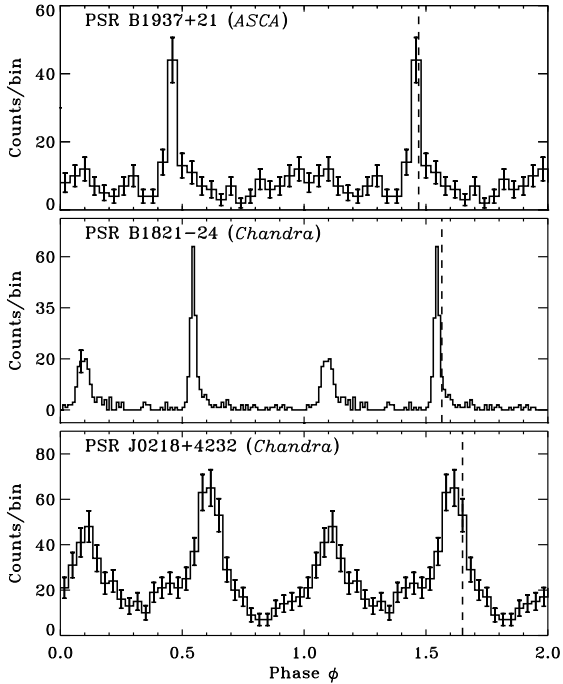


Fig. 6 Pulsed profiles of three nonthermally emitting MSPs. Vertical dashed lines indicate phases of main radio pulses. See Takahashi et al. (2000), Rutledge et al. (2004), and Kuiper et al. (2002) for more details on timing analysis of X-rays from PSRs B1937+21, B1821-24, and J0218+4232 (respectively).

corona above the pulsar provided its magnetic field is strongly different from a centered dipole. The estimated nonthermal (isotropic) luminosities⁵ of these four objects in the 0.2–10 keV range, L^{nonth} , and the corresponding “nonthermal” efficiencies, $\eta^{\text{nonth}} = L^{\text{nonth}}/\dot{E}$, are given in Table 2. Note that a fraction of the X-ray emission detected from the eclipsing pulsar B1957+20, which is thought to ablate its companion in a close binary system with a 9.2-hr orbital period, may be due to an intrabinary shock between the pulsar wind and that of the companion star. The *Chandra* data on this MSP showed an apparent (at a 99% confidence level) modulation of the X-ray emission detected at the pulsar’s position with orbital phase (Stappers et al. 2003), with lowest and highest fluxes during and immediately after eclipse (respectively). Assuming that this flux modulation is genuine, Stappers et al. (2003) obtained a 50% estimate on the contribution of X-ray emission from the intrabinary shock in the total flux detected from the pulsar. This fraction is accounted for in deriving the nonthermal luminosity and efficiency for PSR B1957+20 given in Table 2.

Another prominent feature of the nonthermal emission from three of these MSPs is the shape of the X-ray pulsed profiles, with strong and narrow main pulses and large pulsed fractions f_p ranging from about 65% for

PSR B0218–4232 up to nearly 100% for PSRs B1937+21 and B1821–24. Figure 6 presents the pulsars’ light curves. Nonthermal pulsed emission from these MSPs was also detected up to about 20 keV with *RXTE* (Rots et al. 1998; Kuiper, Hermsen & Stappers 2004; Cusumano et al. 2003). The main X-ray and radio peaks of these pulsars were found to be nearly aligned in phase (based on both *Chandra* and *RXTE* data)⁶. This suggests that nonthermal photons emitted from these MSPs in the radio and X-ray bands are generated in the same (or close) zones, although it still remains unclear where those zones are located: closer to the neutron star surface (as suggested by the polar-cap model of Harding, Usov & Muslimov 2005) or near the pulsar light cylinder (according to the outer-gap model — e.g., Cheng, Ho & Ruderman 1986, Romani 1996). Pulsations of the X-ray flux emitted by PSR B1957+20 have to be detected yet⁷.

3 Thermally emitting MSPs

This is the second group of objects in Table 1 which consists of PSRs J0030+0451, J2124–3358, J1024–0719, and J0437–4715. These MSPs are less energetic in terms of \dot{E} , have longer spin periods and are much closer to Earth. X-ray spectra of the two brightest members of this group, PSRs J0030+0451 and J0437–4715 cannot be fitted with a single PL model, whereas for the other two pulsars such a fit yields too large photon indices, $\Gamma \simeq 3\text{--}4$, and the obtained estimates on hydrogen column density, $n_{\text{H}} \simeq (1\text{--}2) \times 10^{21} \text{ cm}^{-2}$, towards these objects greatly exceed those inferred from independent measurements (Zavlin 2006). A broken-PL model, suggested by Becker & Aschenbach (2002) to interpret the spectra of PSRs J0030+0451 and J0437–4715, results in unrealistic estimates on n_{H} . A model involving a PL and a simple one-temperature thermal component also faces the same problem.

Analyzing *ROSAT* data on PSR J0437–4715, Zavlin & Pavlov (1998) suggested a thermal model implying a nonuniform temperature distribution over PCs. These authors discussed that relativistic particles bombarding magnetic poles of an MSP could heat a region larger than the conventional PC size (see Sec. 1) because the low magnetic field of the pulsar does not prevent the released heat from propagating along the neutron star surface. The applied model assumes two identical PCs on magnetic poles covered with a weakly magnetized hydrogen atmosphere (Zavlin, Pavlov & Shibanov 1996). It also takes into account the GR effects (redshift and bending of photon trajectories near the neutron star surface). In this model the thermal radiation depends on

⁶ Although Takahashi et al. (2001) found from *ASCA* data that the main X-ray and radio pulses of PSR B1937+21 are separated by $\Delta\phi \simeq 0.5$ in phase.

⁷ No results from the *XMM-Newton* observation of this MSP conducted in October 2004 have been reported yet.

⁵ X-ray luminosities of the pulsars discussed in Sections 2 and 3 are derived for the distances given in Table 1.

PC temperature and radius, the neutron star mass-to-radius ratio, which determines the GR effects, and the star geometry (the viewing and magnetic angles, ζ and α , respectively). The sketch shown in Figure 7 illustrates the neutron star geometry and the effect of light bending (see also, e.g., Zavlin, Shibano & Pavlov 1995 for more details on the GR effects on pulsar PC emission). The nonuniform temperature was approximated with a step-like function, referred as PC “core” and “rim”. Observations of PSR J0437–4715 with *Chandra* (Zavlin et al. 2002) and *XMM-Newton* (Zavlin 2006) showed that such a model, supplemented with a PL component of $\Gamma \simeq 2.0$, fits well the spectrum of PSR J0437–4715 up to 10 keV and yields reasonable pulsar parameters as well as n_{H} . The thermal model provides the bulk of the pulsar’s X-ray flux, whereas the PL component prevails only at photon energies $E \gtrsim 3$ keV. A similar (nonuniform PCs plus PL) model works also well on the spectral data of PSR J0030+0451. Figures 8 and 9 demonstrate this. The inferred parameters of the thermal components are: $T_{\text{pc}}^{\text{core}} \simeq 1.4$ and 2.1 MK, $T_{\text{pc}}^{\text{rim}} \simeq 0.5$ and 0.8 MK, $R_{\text{pc}}^{\text{core}} \simeq 0.4$ and 0.1 km, $R_{\text{pc}}^{\text{rim}} \simeq 2.6$ and 1.4 km, for PSRs J0437–4715 and J0030+0451, respectively (in the latter case the PL index was fixed at $\Gamma = 1.5$ because of a poorer data statistics at higher energies). For PSRs J2124–3358 and J1024–0719 the same model yields PC parameters close to those mentioned above, although low quality of the observational data on these two objects at $E > 3$ keV allows one to put only upper limits on intensity of the nonthermal component (Zavlin 2006). The bolometric luminosities of one PC, $L_{\text{bol}}^{\text{pc}}$, and “PC efficiencies”, $\eta^{\text{pc}} = L_{\text{bol}}^{\text{pc}}/\dot{E}$, can be found in Table 2, together with the estimates on L^{nonth} and η^{nonth} for the nonthermal component (or corresponding 1σ upper limits). Upper limits on the luminosity of a possible thermal PC component in the X-ray fluxes of the four nonthermally emitting pulsars (Sec. 2) are also given in Table 2. Note that a more detailed study of possible thermal emission from these four pulsars is hampered by large distances (a few kpc) and, hence, strong interstellar absorption ($n_{\text{H}} \sim [2\text{--}4] \times 10^{21} \text{ cm}^{-2}$) towards these objects.

As alternative to the PC-plus-PL model of the X-ray emission from PSR J0437–4715, Bogdanov, Grindlay & Rybicki (2006) suggested a purely thermal interpretation in which the harder X-ray spectral tail (at $E \gtrsim 3$ keV) is a result of the inverse Compton scattering of soft thermal PC photons by energetic electrons/positrons in an optically thin thermal layer of a temperature $kT_e \sim 150$ keV located presumably in the pulsar’s magnetosphere. However, as existence of such a thermal layer in a pulsar magnetosphere does not seem to be physically supported, this Comptonization interpretation remains rather questionable.

X-ray emission from all these four thermally emitting MSPs is pulsed, with pulsed fraction ranging from about 35% up to 50% (Becker & Aschenbach 2002; Zavlin

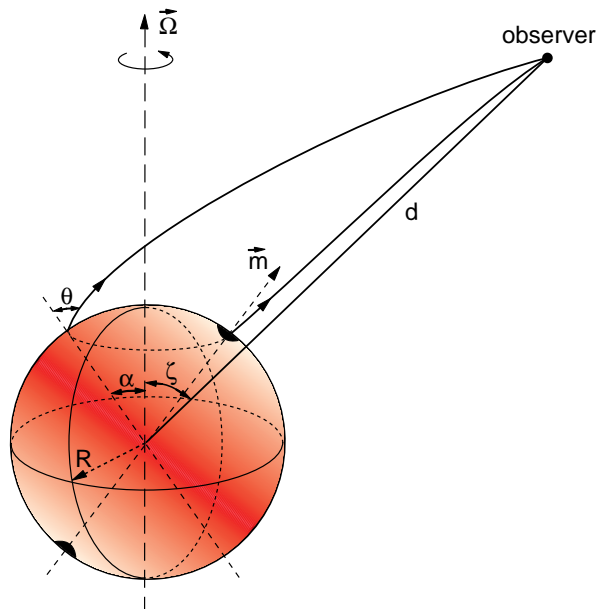


Fig. 7 Sketch illustrating bending of photon trajectories in a strong gravitational field near the surface of a neutron star with rotational and magnetic axes Ω and m , and viewing and magnetic angles ζ and α (respectively).

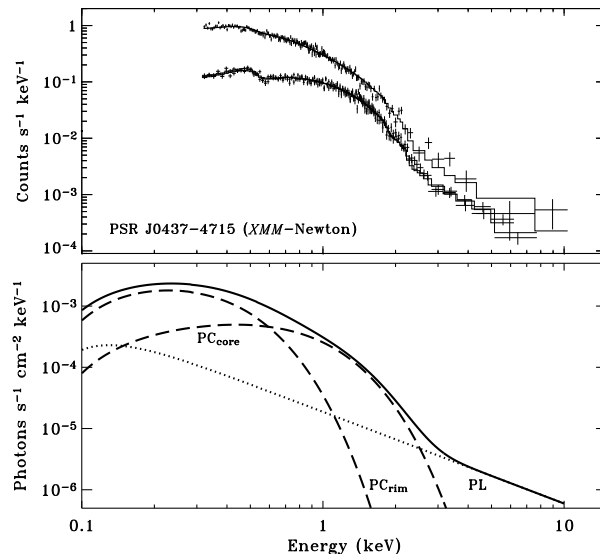
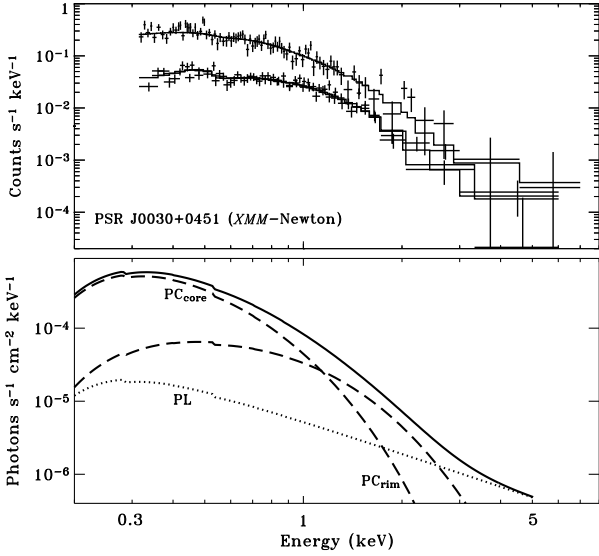


Fig. 8 X-ray spectra of PSR J0437–4715 as detected with the *XMM-Newton* EPIC-pn and MOS instruments (crosses). The solid curves show a best fitting model, PL (dots) plus a two-temperature PC component (dashes), “core” and “rim” (see Sec. 3).

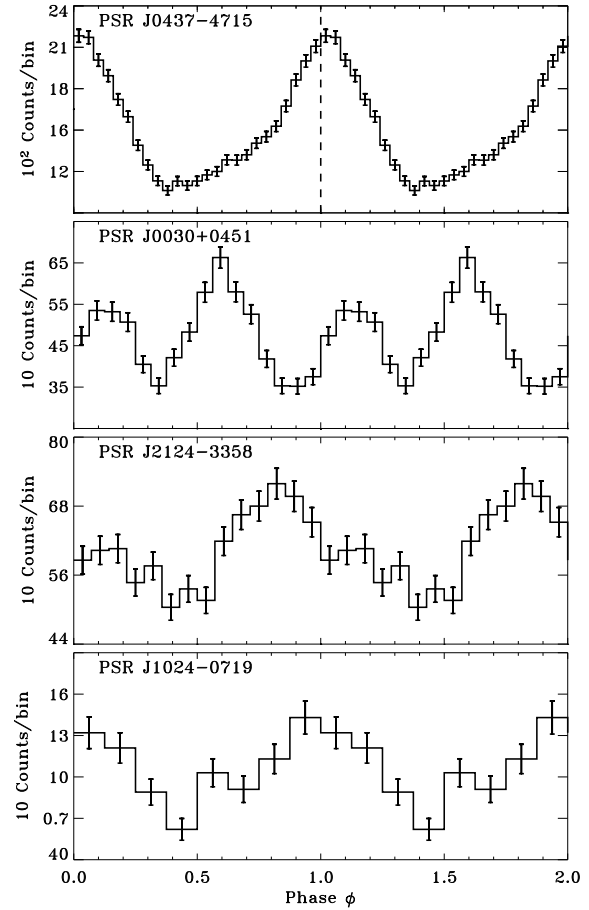
2006). The pulsed profiles of PSRs J0437–4715, J2124–3358, and J1024–0719 are rather similar in shape, with single broad pulses, whereas the light curve of PSR J0030+0451 exhibits two pulses per period separated by $\Delta\phi \simeq 0.5$ in phase. This indicates that the geometry of PSR J0030+0451 (the angles ζ and α) is different from those of the three others. For example, in the framework of the conventional pulsar model with the magnetic dipole

Table 2 X-ray luminosities of eight MSPs

PSR	$\text{Log } L^{\text{nonth}}$ (erg s^{-1})	$\text{Log } L_{\text{bpl}}^{\text{pc}}$ (erg s^{-1})	$\text{Log } \eta^{\text{nonth}}$	$\text{Log } \eta^{\text{pc}}$
B1937+21	32.8	< 31.5	-3.2	< -4.5
B1957+20	31.5	< 30.4	-3.5	< -4.6
J0218+4232	32.6	< 31.0	-2.8	< -4.4
B1821-24	32.7	< 32.0	-3.6	< -4.3
J0030+0451	29.8	30.3	-3.7	-3.2
J2124-3358	< 29.0	30.0	< -4.6	-3.6
J1024-0719	< 28.9	29.3	> -3.6
J0437-4715	29.7	30.2	-3.8	-3.3

**Fig. 9** Same as in Fig. 8 for PSR J0030+0451.

at the neutron star center, PSR J0030+0451 can be a nearly orthogonal rotator (i.e., $\zeta \simeq \alpha \simeq 90^\circ$) with two pulses in its light curve being due to contributions from two PCs seen during the pulsar’s rotation. For the other MSPs, the bulk of the detected X-ray fluxes is expected to come mostly from one PC. However, the X-ray pulses of PSRs J0437-4715, J1024-0719, and J2124-3358 are clearly asymmetric, with a longer rise and a faster decay for the former two MSPs and with the opposite behavior for the latter two MSPs. None of these shapes can be explained by a simple axisymmetric temperature distribution. A feasible interpretation is that the observed asymmetry in the pulsed profiles of these three MSPs is caused by contribution of the nonthermal component whose peak is shifted in phase with respect to the pulse of the thermal emission. Results of the energy-resolved timing and phase-resolved spectroscopy on the *XMM-Newton* data on PSR J0437-4715 support this explanation (Zavlin 2006). For PSR J2124-3358, there may be an alternative interpretation of the shape of the pulsar’s light curve: the steeper rise and longer trail could be caused by relativistic effects (in particular, the Doppler

**Fig. 10** Pulsed profiles of thermally emitting MSPs obtained from *XMM-Newton* observations (Zavlin 2006). The vertical dashed line in the upper panel indicates phase of a radio pulse of PSR J0437-4715 (see Sec. 3 for details).

boost) in fast rotating pulsars (Braje, Romani & Rauch 2000), although it then should be understood why these effects are not seen in the pulse profiles of the other three MSPs whose the spin periods close to that of PSR J2124-3358 (Table 1). Another way to attempt to explain the observed light curves is to involve a model with a decentered magnetic dipole (or another magnetic field config-

uration — see the presentation by S. Zane at this conference), what has not been done yet for interpreting pulsed X-ray emission from MSPs. In any case, to produce a pulsed fraction at a level of $f_p \gtrsim 30\%$, thermal emission has to be anisotropic, as predicted by neutron star atmosphere models, to counteract the effect of light bending near the star surface on pulsations of the thermal flux (Zavlin, Shibano & Pavlov 1995). So far, the difference in phases between radio and X-ray pulses was determined only for PSR J0437–4715 based on *Chandra* data (Zavlin et al. 2002; see also Fig. 10). As the bulk of the X-ray flux from this pulsar is of the thermal PC origin, the small difference in phases of the radio and X-ray peaks suggests that the pulsar’s radio emission is generated close to the neutron star surface, unless the effects of field-line sweepback and/or aberration cancel the travel-time difference.

4 More X-ray emitting MSPs

Three pulsars, J0034–0534, J0751+1807, and J1012+5307, are examples of MSPs firmly detected in X-rays but whose radiative properties remain uncertain. X-ray observations of these objects were not long enough to provide data suitable for discriminating among various spectral models. Those data could be equally well fitted with a PL model of $\Gamma \sim 1.7$ or a thermal (blackbody) model of a temperature of ~ 3 MK (see Webb et al. 2004 and Zavlin 2006). Estimates on the total flux are the only rather reliable X-ray characteristics available for these objects. Table 3 presents the main pulsar parameters⁸ together with the estimated X-ray luminosities in the 0.2–10 keV range, L_X , and corresponding efficiencies, $\eta_X = L_X/\dot{E}$. In terms of the spin-down power \dot{E} , PSRs J0751+1807 and J1012+5307 join the four pulsars exhibiting thermal PC emission (Sec. 3), while PSR J0034–0534 seems to be more energetic and closer to the first group of the non-thermally emitting MSPs (Sec. 2). On the other hand, PSR J0034–0534 is most “underluminous”, its luminosity, $L_X \simeq 0.5 \times 10^{30}$ erg s^{−1}, is as low as that estimated for PSR J1024–0719, the least energetic pulsar among the MSPs discussed in Sections 2–4. The X-ray efficiency of PSR J0034–0534, $\eta_X \simeq 1.6 \times 10^{-5}$, is smaller at least by an order of magnitude than those measured for the other MSPs (Tables 2 and 3). However, it is worth mentioning that the estimate on \dot{E} given in Table 2 for PSR J0034–0534 assumes that the intrinsic period derivative of the pulsar is as directly measured in radio observations, i.e., without accounting for the Shklovskii effect on \dot{P} due to pulsar proper motion (Shklovskii 1970). The proper motion of PSR J0034–0534 has not been determined yet. Still, it is reasonable to assume that the trans-

verse component of the pulsar’s velocity may be about $100 (d/0.54 \text{ kpc})^{1/2}$ km s^{−1} (what is not unusual for a binary MSP — see Lommen et al. 2006). Then, its intrinsic \dot{P} and, hence, \dot{E} would be reduced by a factor of 10, making the pulsar’s X-ray efficiency similar to those found for the MSPs with $\dot{E} < 10^{34}$ erg s^{−1}.

5 MSPs and their nebulae

Relativistic pulsar winds, which carry away pulsar rotational energy, interact with ambient medium, that is expected to form PWNe detectable at different wavelengths. In X-rays, about 30 PWNe are currently known (see Kaspi, Roberts & Harding 2006, Gaensler & Slane 2006 and Kargaltsev & Pavlov 2006 for reviews, as well as electronic PWN catalogs⁹), thanks mainly to the superb spatial resolution of *Chandra* (see the presentation by Weisskopf et al. at this conference for a review). The observed X-ray PWNe are diverse in properties. Some of them are of a torus-like structure with jets along the symmetry axis (which apparently coincides with the pulsar’s spin axis, as suggested for the young Crab and Vela pulsars — Weisskopf et al. 2000, Pavlov et al. 2003). Several others have a cometary-like shape caused by the pulsar motion. The “Mouse” PWN powered by PSR J1747–2958 (Gaensler et al. 2004) is confined within a bow-shaped boundary without a shell-like structure. X-ray PWNe associated with PSR B1757–24 (Kaspi et al. 2001), J1509–5859 and J1809–1917 (Sanwal, Pavlov & Garmire 2005), and the Geminga pulsar (Caraveo et al. 2003; De Luca et al. 2006; Pavlov, Sanwal & Zavlin 2006) have elongated structures that look like “trails” (or “wakes”) behind the moving pulsars. These tails could be pulsar jets confined by toroidal magnetic fields, or they could be associated with shocked relativistic wind confined by the ram pressure of the surrounding interstellar medium. Two X-ray nebulae produced by the MSPs, B1957+20 (Stappers et al. 2003) and J2124–3358 (Hui & Becker 2006), belong to the latter group of PWNe. These are shown in Figures 11 and 12. Besides, optical observations revealed H α bow-shocks surrounding these two pulsars (sketched with dashed curves in Figs. 11 and 12). Both X-ray PWNe have a form of a 20''-long tail, although there is a striking difference between their shapes. The H α bow-shock and X-ray tail of PSR B1957+20 are fairly symmetric, with the symmetry axis being nearly aligned with the direction of the pulsar’s proper motion (Fig. 11). For PSR J2124–3358, both the bow-shock and the X-ray tail are bent and highly asymmetric with respect to the proper motion vector (Fig. 12). Gaensler, John & Stappers (2002) argued that such an unusual shape of a PWN could be caused by a combination of effects associated with anisotropy of the

⁸ The distance to PSR J0751+1807 is derived from the pulsar’s parallax (Nice et al. 2005), whereas the other two estimates are obtained from the pulsars’ dispersion measures and the NE2001 model.

⁹ <http://www.astro.psu.edu/users/green/psrdatabase/psrcat.htm>, <http://www.physics.mcgill.ca/~pulsar/pwncat.html>

Table 3 Three MSPs with estimates on X-ray flux

PSR	P (ms)	d (kpc)	τ (Gyr)	$\log \dot{E}$ (erg s^{-1})	$\log L_X$ (erg s^{-1})	$\log \eta_X$
J0034-0534	1.88	0.54	6.0	34.5	29.7	-4.8
J0751+1807	3.48	0.63	7.7	33.8	30.3	-3.5
J1012+5307	5.26	0.41	8.6	33.4	30.4	-3.0

pulsar wind and density nonuniformity of the surrounding medium. Analyzing the properties of the X-ray PWN of PSR B1957+20, Stappers et al. (2003) speculated that the efficiency with which relativistic particles are accelerated in the pulsar’s wind can be as high as those inferred for young pulsars with much stronger surface magnetic fields. Comparing ratios of X-ray luminosities of tail-like PWNs to pulsar spin-down energies may be considered as an additional evidence in favor of this conclusion: the ratio, $L_X/\dot{E} \sim 10^{-4}$, estimated for the tail associated with PSR B1957+20 is very close to that found for the nebula produced by the 16-kyr-old PSR B1757-24 (Kaspi et al. 2001) and greatly exceeds those inferred for the Geminga’s tail, $\sim 4 \times 10^{-6}$ (Pavlov, Sanwal & Zavlin 2006) and the Vela’s southeast jet, $\sim 1 \times 10^{-6}$ (Pavlov et al. 2003). Contrary to these two objects, the third MSP whose supersonic motion through the ambient medium causes an H_α bow-shock, J0437-4715, has not been found to power an X-ray nebula, suggesting a very low magnetic field in the expected PWN region (Zavlin et al. 2002). No an X-ray PWN associated with the most energetic MSPs B1937+21 has been detected in a deep *Chandra* observation of this pulsar (Kuiper et al. 2006).

6 Summarizing remarks

X-ray observations of the MSPs discussed in this paper and those located in the globular clusters (Bogdanov et al. 2006) revealed that most of them emit predominantly thermal PC emission with a luminosity of $L_{\text{bol}}^{\text{pc}} \sim 10^{30-31} \text{ erg s}^{-1}$ and “PC efficiency” of $\eta^{\text{pc}} \sim 10^{-4-10^{-3}}$. It is worth noting that these estimates on η^{pc} are close to that derived for the old ordinary pulsar B0950+08 ($\tau \simeq 17 \text{ Myr}$, $P \simeq 253 \text{ ms}$, $\dot{E} \simeq 6 \times 10^{32} \text{ erg s}^{-1}$), $\eta^{\text{pc}} \simeq 2.4 \times 10^{-4}$ (Zavlin & Pavlov 2004), suggesting that heating mechanisms in ordinary and rapidly spinning pulsars may be quite similar. Comparing pulsar parameters of the MSPs with detected X-ray radiation shows that the four MSPs with nonthermal radiation possess much large values of \dot{E} , by at least a factor of 50, than those estimated for the thermally emitting pulsars. The numbers presented in Table 2 indicate that the larger is \dot{E} , the higher is the “nonthermal” efficiency η^{nonth} , whereas the opposite tendency is apparent for η^{pc} . A similar behavior of η^{pc} follows from results of the theoretical

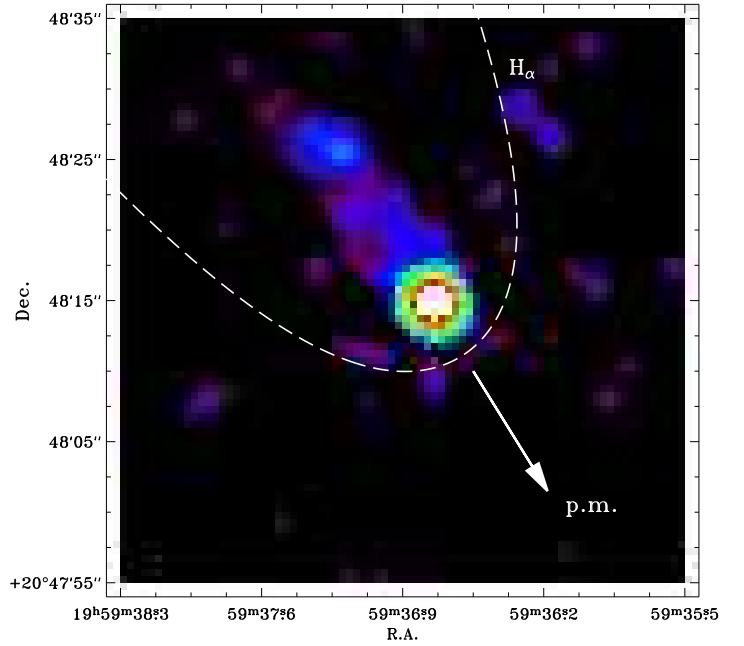


Fig. 11 *Chandra* image of PSR B1957+20 and its tail-like X-ray PWN. The dashed curve sketches the H_α nebula associated with the pulsar. The arrow indicates the direction of the pulsar’s proper motion.

modeling of the PC heating by returning positrons produced through curvature radiation and inverse Compton scattering (see Figs. 7 and 8 in Harding & Muslimov 2001 and 2002, respectively, with account for the relation $\dot{E} \sim \tau^{-[n+1]/[n-1]} = \tau^{-2}$, for the magneto-dipole braking index $n = 3$). In addition, high luminosity of the nonthermal emission may be associated with large values of the magnetic field at the pulsar light cylinder (Saito et al. 1997), $B_{\text{lc}} = B_{\text{surf}} [2\pi R_{\text{NS}}/cP]^3$. Indeed, the nonthermally emitting MSPs possess magnetic fields, $B_{\text{lc}} \sim (0.3-1) \times 10^6 \text{ G}$, close to that of the Crab pulsar ($\sim 1 \times 10^6 \text{ G}$) and exceeding those in the MSPs with thermal emission (as well as in PSRs J0751+1807 and J1012+5307), $B_{\text{lc}} \sim 0.03 \times 10^6 \text{ G}$, at least by an order of magnitude. This may indicate that the nonthermal radiation of MSPs is generated in emission zone(s) close to the light cylinder (as predicted by the outer-gap pulsar models) and that B_{lc} is an important parameter governing the

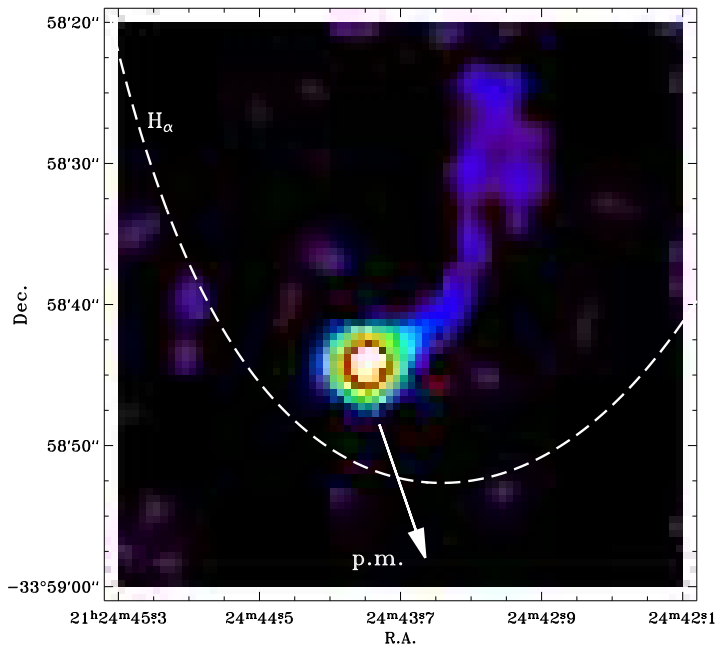


Fig. 12 Same as in Fig. 11 for PSR J2124–3358.

magnetospheric activity. On the other hand, a model by Harding, Usov & Muslimov (2005) for acceleration and pair cascades on open field lines close to pulsar PCs describes rather well the spectrum of PSR J0218+4232 observed from X-rays through γ -rays. Hence, at the present stage, neither of the two models (outer-gap or polar-cap) of the nonthermal emission of MSPs could be regarded as more favorable. Besides, one cannot rule out that the pulsar spin period also affects η^{nonth} — the MSPs of the first group have shorter periods than those of the other four pulsars (Table 1). Definitely, a bigger sample of X-ray emitting MSPs is required to draw more conclusive speculations.

The results of Section 3 point out that PCs of MSPs are likely nonuniform, with temperatures decreasing by a factor of 2–3 from the PC center down to its edge. There have not been yet reliable calculations of the temperature distribution around the pulsar magnetic poles. Hence, sophisticated theoretical models of PC heating and temperature distribution are required for further investigation of thermal X-ray emission from MSPs.

As shown by Pavlov & Zavlin (1997), modeling of an X-ray pulsed profile can yield constraints on the pulsar mass-to-radius ratio as well as its geometry. To do that, more elaborated models of magnetospheric pulsed emission and data of a better quality at higher energies are required to disentangle nonthermal and thermal components.

Chandra and *XMM-Newton* provided remarkable detections of two double-neutron-star binary systems with

MSPs as companions, J0737–3039 and J1537+1155 (Campana, Possenti & Burgay 2004; McLaughlin et al. 2004; Pellizzioni et al. 2004; Kargaltsev, Pavlov & Garmire 2006). Although the collected data are of a rather scanty statistics, one could conclude that the inferred X-ray spectra and luminosities of these two system are similar, suggesting the same mechanisms generating the detected radiation. Among various interpretations proposed, the most plausible one is that the observed emission consists of a thermal PC component emitted by the MSPs plus nonthermal X-rays from the interaction of the pulsar winds with the neutron star companions. This interpretation explains a gap observed in the orbital dependence of the X-ray flux emitted by the highly eccentric J1537+1155 system (Kargaltsev, Pavlov & Garmire 2006). To investigate these systems in more detail, a phase-resolved spectroscopy on X-ray data of a better quality is required to separate possible components in X-rays from these objects. Further observations are expected to constrain both the properties of the pulsar winds and those of the pulsars themselves in these (and other) double-neutron-star systems.

So far, only one MSP, J0437–4715, has been observed and detected in the *UV/FUV* band (Kargaltsev, Pavlov & Romani 2004). The shape of the inferred spectrum suggests thermal emission from the whole neutron star surface of a surprisingly high temperature of about 0.1 MK. A heating mechanism should be operating in a Gyrod neutron star to keep its surface at such temperature. As discussed by Kargaltsev, Pavlov & Romani (2004), among several possible mechanisms (both internal and external), chemical heating (Reisenegger 1995) and frictional heating (e.g., Cheng et al. 1992) of the neutron star core are the most plausible options. To understand thermal evolution of neutron stars, more MSPs (e.g., the other three pulsars discussed in Sec. 3) and close ordinary old pulsars (PSR B0950+08 is one of the best candidates — Zavlin & Pavlov 2004) should be observed in the *UV/FUV* band. The example of PSR J0437–4715 shows that such an observational program would be feasible.

As a final remark, it is worth mentioning that so far all known isolated (non-accreting) MSPs were first discovered in radio. In X-rays a first attempt to find millisecond pulsations from an isolated compact object was done by Zavlin & Pavlov (2006) who suggested that the most famous (and intriguing) member of the group of the “dim” isolated, radio-quiete, and thermally emitting neutron stars discovered with *ROSAT* (see the presentation by F. Haberl at this conference), RX J1856.5–3754, could be an MSP (see Pavlov & Zavlin 2003 for a discussion). One of the reasons to look for millisecond pulsations was the fact that the X-ray flux detected from this object in deep observations with *Chandra* and *XMM-Newton* revealed no pulsations at periods above 20 ms (the period range to which those observational data were sensitive), with a stringent upper limit on the pulsed fraction

$f_p < 1.3\%$. To check the MSP hypothesis, a deep XMM-Newton observation of RX J1856.5–3754 in an instrumental model with a temporal resolution of 0.03 ms was conducted in April 2004. Despite a very large number of source counts collected in this observation ($\sim 2 \times 10^5$), no significant pulsations were found at periods in the range $P = 1\text{--}20$ ms. The derived 1σ upper limit on the pulsed flux for this period range is $f_p < 2.1\%$. This non-detection virtually excludes the MSP interpretation for RX J1856.5–3754 and supports alternative hypotheses of a very special neutron star's geometry and/or a very long spin period ($P \gtrsim 10$ hr).

Acknowledgements The author thanks George Pavlov for useful discussions. This work is supported by a NASA Research Associateship Award at NASA Marshall Space Flight Center. The study of RX J1856.5–3754 with XMM-Newton was made possible through the NASA grant NNG04GI801G.

References

1. Alpar M.A., Cheng A.F., Ruderman M.A., et al., *Nature*, **300**, 728 (1982)
2. Arons J., Tavani M., *ApJ*, **403**, 249 (1993)
3. Backer D.C., Kulkarni S.R., Heiles C., et al., *Nature*, **300**, 615 (1982)
4. Becker W., Trümper J., *Nature*, **365**, 528 (1993)
5. Becker W., Aschenbach B., In: *Neutron Stars, Pulsars and Supernova Remnants*, ed. W. Becker, H. Lesch & J. Trümper, MPE Report 278, p. 64 (2002)
6. Becker W., Schwarz D.A., Pavlov G.G., et al., *ApJ*, **594**, 798 (2003)
7. Bogdanov S., Grindlay J.E., Heinke C.O., et al., *ApJ*, **646**, 1104 (2006)
8. Bogdanov S., Grindlay J.E., Rybicki G.B., *ApJ*, submitted (2006; astro-ph/0605273)
9. Braje T.M., Romani R.W., Rauch K.P., *ApJ*, **531**, 447 (2000)
10. Campana S., Possentti A., Burgay M., *ApJL*, **613**, 53 (2004)
12. Caraveo P.A., Bignami G.F., De Luca A., et al., *Science*, **301**, 1345 (2005)
22. Cheng K.S., Ho C., Ruderman M., *ApJ*, **300**, 500 (1986)
45. Cheng K.S., Chau W.Y., Zhang J.L., et al., *ApJ*, **396**, 135 (1992)
14. Cordes J.M., Lazio T.J.W., preprint, (2003; astro-ph/0301598)
15. Cumming A., In: *Binary Radio Pulsars*, ed. F.A. Rasio & I.H. Stairs, ASP Conference Series 238 (San Francisco: ASP), p. 311 (2005)
16. Cusumano G., Hermsen W., Kramer M., et al., *A&A*, **410**, L9 (2003)
17. De Luca A., Caraveo P.A., Mattana F., et al., *A&A*, **445**, L9 (2006)
18. Gaensler B.M., Jones D.H., Stappers B.W., *ApJ*, **580**, L137 (2002)
19. Gaensler B.M., van der Swaluw E., Camilo F., et al., *ApJ*, **616**, 383 (2004)
20. Gaensler B.M., Slane P.O., *Ann. Rev. Astron. Astrophys.*, **44**, 17 (2006)
22. Harding A.K., Muslimov A.G., *ApJ*, **556**, 987 (2001)
22. Harding A.K., Muslimov A.G., *ApJ*, **568**, 862 (2002)
23. Harding A.K., Usov V.V., Muslimov A.G., *ApJ*, **622**, 531 (2005)
24. Hotan A.W., Bailes M., Ord S.M., *MNRAS*, **369**, 1502 (2006)
25. Hui C.Y., Becker W., *A&A*, **448**, L13 (2006)
26. Kargaltsev O.Y., Pavlov G.G., Romani R.W., *ApJ*, **602**, 327 (2004)
27. Kargaltsev O.Y., Pavlov G.G., in preparation (2006)
28. Kargaltsev O.Y., Pavlov G.G., Garmire G.P., *ApJ*, **646**, 1139 (2006)
29. Kaspi V.M., Roberts M.S.E., Harding A.K., In: *Compact Stellar X-ray Sources*, ed. W.H.G. Lewin & M. van der Klis, Cambridge University Press, p. 279 (2006)
30. Kaspi V.M., Gotthelf E.V., Gaensler B.M., et al., *ApJL*, **562**, 163 (2001)
31. Kuiper L., Hermsen W., Verbunt F., et al., *A&A*, **359**, 615 (2000)
32. Kuiper L., Hermsen W., Verbunt F., et al., *ApJ*, **577**, 917 (2002)
33. Kuiper L., Hermsen W., Stappers B., *Ad. Sp. Res.*, **33**, 507 (2004)
34. Kuiper L., et al., *A&A*, submitted (2006)
35. Lommen A.N., Kipporn R., Nice D.J., et al., *ApJ*, **642**, 1012 (2006)
36. Manchester R.N., Hobbs G.B., Teoh A., et al., *AJ*, **129**, 1993 (2005)
37. McLaughlin M.A., Camilo F., Burgay M., et al., *ApJL*, **605**, 41 (2004)
38. Nicastro L., Cusumano G., Löhmer O., et al., *A&A*, **413**, 1065 (2004)
39. Nice D.J., Splaver E.M., Stairs I.H., et al., *ApJ*, **634**, 1242 (2005)
40. Pavlov G.G., Zavlin V.E., *ApJL*, **490**, 91 (1997)
41. Pavlov G.G., Zavlin V.E., In: *The XXI Texas Symposium on Relativistic Astrophysics*, ed. R. Bandiera, R. Maiolino & F. Mannucci, World Science Publishing, p. 319 (2003)
42. Pavlov G.G., Teter M.A., Kargaltsev O.Y., et al., *ApJ*, **591**, 1157 (2003)
43. Pavlov G.G., Sanwal D., Zavlin V.E., *ApJ*, **643**, 1146 (2006)
44. Pellizzoni A., De Luca A., Mereghetti S., et al., *ApJL*, **612**, 49 (2004)
45. Reisenegger A., *ApJ*, **442**, 749 (1995)
46. Romani R.W., *ApJ*, **470**, 469 (1996)
47. Rots A.H., Jahoda K., Makomb D.J., et al., *ApJ*, **501**, 749 (1998)
48. Rutledge R.E., Fox D.W., Kulkarni S.R., et al., *ApJ*, **613**, 522 (2004)
49. Saito Y., Kawai N., Kamae T., et al., *ApJL*, **447**, 37 (1997)
50. Sanwal D., Pavlov G.G., Garmire G.P., *AAS*, **206**, 43.02 (2005)
51. Shklovskii I.S., *Sov. Astr.*, **13**, 562 (1970)
52. Stappers B.W., Gaensler B.M., Kaspi V.M., et al., *Science*, **299**, 1372 (2003)
53. Takahashi M., Shibata S., Torii K., et al. *ApJ*, **554**, 316 (2001)
55. Webb N.A., Olive J.-F., Barret D., *A&A*, **417**, 181 (2004)
55. Webb N.A., Olive J.-F., Barret D., et al., *A&A*, **419**, 269 (2004)
56. Weisskopf M.C., Hester J.J., Tennant A.F., et al., *ApJL*, **536**, 81 (2000)
57. Wijnands R., *Nuc. Phys. B*, **132**, 486 (2004)
58. Zavlin V.E., Shibanov Yu.A., Pavlov G.G., *Astron. Let.*, **21**, 149 (1995)
59. Zavlin V.E., Pavlov G.G., Shibanov Yu.A., *A&A*, **315**, 141 (1996)
60. Zavlin V.E., Pavlov G.G., *A&A*, **329**, 583 (1998)
61. Zavlin V.E., Pavlov G.G., Sanwal, D., et al., *ApJ*, **569**, 894 (2002)
62. Zavlin V.E., Pavlov G.G., *ApJ*, **616**, 452 (2004)
63. Zavlin V.E., *ApJ*, **638**, 951 (2006)
64. Zavlin V.E., Pavlov G.G., in preparation (2006)